PETROPHYSICAL ANALYSIS OF PICEANCE BASIN TIGHT GAS SANDSTONES, NW COLORADO, TO DISTINGUISH WET SANDS FROM GAS-BEARING SANDS, AND TO CATEGORIZE ROCK QUALITY VARIATION BY INCORPORATING CAPILLARY PRESSURE INTERPRETATIONS

Michael Holmes, Antony M. Holmes, and Dominic I. Holmes, Digital Formation, Inc.

ABSTRACT

In the southern part of the Piceance Basin, NW Colorado, gas-bearing non-marine sandstones of the Williams Fork formation of the Mesa Verde Group occupy a gross interval ranging from 1700 feet to 2400 feet thick. Above this continuous gas column is a transition zone, about 1000 feet thick, where some of the sandstones are wet and contain relatively fresh water, and some are gas-bearing. When completing wells, it is critical to reliably distinguish between wet and gas-bearing sandstones, both of which can have high resistivity response.

Within the continuous gas column, porosities range from 5% to 15%, and average about 10%. Matrix permeability is mostly less than 0.1 md. Some of the sandstones, have permeability to gas that is so low that commercial production from these levels is unlikely.

This paper is a study of sandstone properties of the Williams Fork formation to address the two issues outlined above.

- Distinction between fresh water-wet sandstones and gas-bearing sandstones of the upper transition zone.
- Petrophysical analysis of sandstones in the continuous gas column, to differentiate intervals with higher matrix permeability from intervals with lower matrix permeability.

To examine the first problem, a technique is described by which density and neutron log responses can be used to quantify gas saturation that does not require knowledge of water resistivity. This approach is used to distinguish between gas-bearing and wet sandstones within the transition zone of the upper part of the Williams Fork formation.

To examine the second problem, a different approach combines core-measured capillary pressure measurements, core-measured permeability and porosity, with petrophysical definition of saturation vs. height profiles for the continuous gas column. One of the products of the analysis is a continuous profile of the changing matrix permeability in the sandstones, as a consequence of rock property variation. Once the model is verified by comparison with core data, it can be applied to wells where no core data exists. This allows for a reservoir-wide distinction between sandstones with higher permeability (potentially commercial) from those with lower permeability (probably non-commercial).

Results from the analysis of thirteen wells are presented. Three of the wells (MWX-1, MWX-2, MWX-3 – all close to the town of Rulison) are from the extensive Gas Research Institute study which has a core database of capillary pressures together with extensive porosity, permeability, and water saturation measurements for most of the sandstones in the Williams Fork formation. Results of modeling these 3 wells have been applied to 10 wells from the Grand Valley, Parachute and Rulison Fields.

INTRODUCTION - GEOLOGIC BACKGROUND

Gas production in the southern part of the Piceance Basin is primarily from non-marine sandstones of the Upper Cretaceous Williams Fork formation. Figure 1 shows an area map and Figure 2 a location map, including well locations of the 13 wells

included in this study, and Figure 3 is a stratigraphic column for the Williams Fork and adjacent formations.

Figure 1: *Location map of Grand Valley, Parachute, Rulison and Mamm Creek Field, Southern Piceance Basin.*

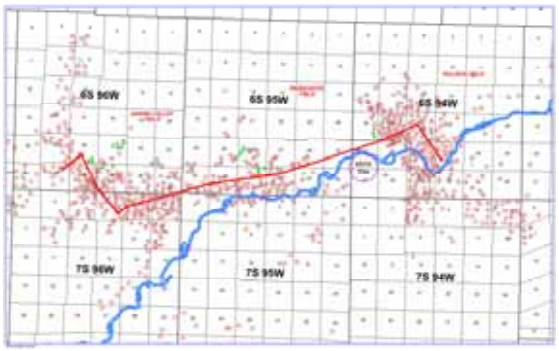

Figure 2: *Locations of the wells in the Piceance Basin used in this study.*

Drilled depths to the top of gas-bearing sandstones ranges from about 2500 feet in the Grand Valley Field to about 5800 feet in the Rulison Field. Thickness of the gross gas productive interval ranges from 1700 feet to 2400 feet. Reservoir pressure ranges from hydrostatic (0.43 psi per foot) near the top of the gas-saturated interval to as high as 0.8 psi per foot at the base of the Williams Fork formation in the Rulison Field.

Source of the gas is primarily the coals in the Cameo interval, but the underlying Mancos Shale also contributes to the gas resource.

The Williams Fork reservoirs are mostly lenticular fluvial sandstones, which show poor lateral continuity from one well to the next (Cumella and Ostby, 2003). Above the continuous gas column is the transition zone containing both wet sandstone intervals as well as gas-filled sandstones.

Symbol	Description
S_W	Water Saturation
R_W	Water Resistivity
P_{ce}	Pore Entry Pressure
P_{cmc}	Capillary Pressure at Model Change
S_{Wmc}	Water Saturation at Model Change
Hyp 1	Shape of Capillary Pressure Curve for Larger Pores
Hyp 2	Shape of Capillary Pressure Curve for Smaller Pores
S_{Wi}	Irreducible Water Saturation
h	Thickness
k	Permeability
Phi	Porosity
EUR	Estimated Ultimate Recovery – from well performance analysis
S_g	Gas Saturation

Table 1: *Description of symbols used in this paper.*

PETROPHYSICAL DISTINCTION BETWEEN WET AND GAS-BEARING SANDSTONESCONCLUSIONS

Above the continuous gas saturated interval are inter-bedded water-bearing sandstones and gas-bearing sandstones. Both types of sandstone have relatively high resistivity, usually from 30 to 50 ohm-meters, due to one of the following reasons:

- Relatively low water resistivity (Rw) accompanied by high gas saturation.
- Much higher water resistivity (Rw) with little or no gas saturation.

Water resistivity of the mostly wet sandstones is about 0.3 ohm-meters as compared to the gas-bearing sandstones, whose water resistivity is about 0.15 ohm-meters.

Qualitative distinction between wet and gas-bearing sandstones is possible by examining density/neutron log responses. If the two curves are plotted using an appropriate lithology transform, wet sandstones should show no "crossover" (suppression of the neutron log in the presence of gas), whereas gas-bearing sandstones will show crossover.

Gas saturation can be quantified, using porosity logs alone, by creating pseudo-porosity logs as follows:

1. Determine clean, wet, formation matrix, and shale properties from a density/neutron cross-plot. For this study, we used sandstones high in the Williams Fork that were several hundred

feet above the top continuous gas column, in sandstones most likely to be wet. Matrix properties for these wet sandstones are calcareous sandstone and a grain density of 2.68 gm per cc.

2. Calculate total porosity from the density/neutron cross-plot for the entire interval of interest. This calculation is relatively independent of fluid content (gas vs. water).

3. Calculate effective porosity by subtracting shale contribution:

$$Total\ Porosity = Effective\ Porosity + V_{SH} \times Shale\ Porosity$$

V_{SH} = volume of shale from the gamma ray log

Calculate pseudo-density and pseudo-neutron logs, level-by-level, knowing porosity, for a full range of assumed gas saturation. For the density log, and neglecting shale, the equation used:

$$Pseudo - Rho_B = Rho_{Matrix} \times (1 - Porosity) + (Porosity \times Rho_{Fluid})$$

Pseudo-RhoB = pseudo-density in gm per cc
RhoMatrix = matrix density
RhoFluid = fluid density
As gas saturation is varied, fluid density will vary as follows:

$$Fluid\ Density = (Gas\ Saturation \times Gas\ Density) + (1 - Gas\ Saturation) \times Water\ Density$$

For the neutron logs, the service companies publish charts showing the effect of varying gas saturation on neutron response. Gas contains less hydrogen than water, so neutron porosity is suppressed in the presence of gas, as compared with a wet formation (Schlumberger 1995). Influences of shale were correctly accounted for in the final calculations.

4. Compare actual density and neutron log responses with the pseudo curves, level-by-level. Where the actual curve crosses the pseudo curve, a quantitative estimate of gas saturation for each porosity log is available.

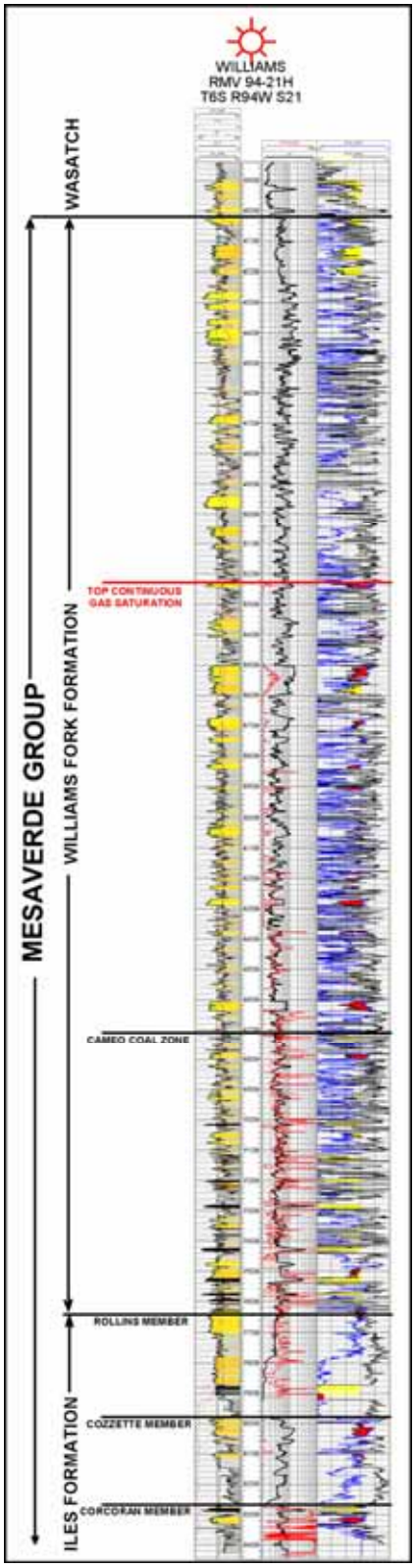

Figure 3: *Type Log for the Mesa Verde Group in the Southern Piceance Basin.*

Figure 4 is a schematic showing how gas saturation can be determined using this methodology. If both density and neutron logs show no gas saturation, then water saturation of 100% is suggested, regardless of resistivity interpretation. If the porosity logs show some degree of gas saturation then either the levels are potentially gas productive or small volumes of residual gas remain. When porosity logs show comparable volumes of gas to resistivity modeling, then the probability of commercial gas production increases.

PETROPHYSICS COMBINED WITH CAPILLARY PRESSURE MODELING OF THE CONTINUOUS GAS COLUMN

This technique involves techniques we have developed and patented involving the combination of capillary pressure measurements on core samples with petrophysical calculations.

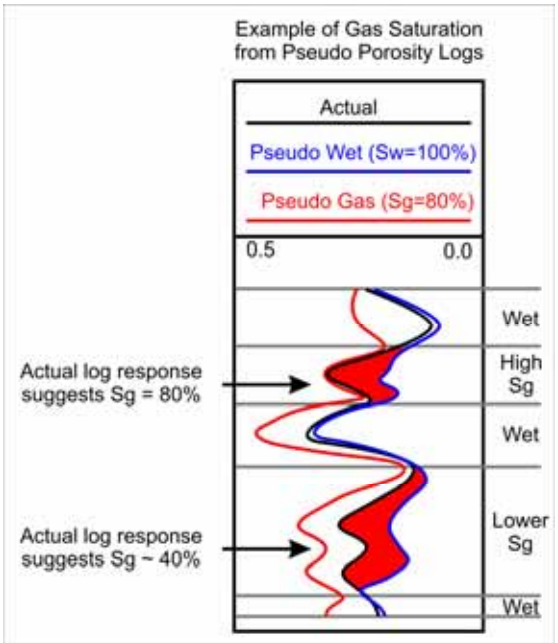

Figure 4: *Schematic diagram to show the application of porosity logs to distinguish between wet rocks and gas-bearing rocks.*

From extensive examination of a large number of reservoirs worldwide, both oil and gas, clastics and carbonates, and covering a wide range of porosity and permeability, we have derived a deterministic saturation/height model that can be compared with petrophysical calculations.

A representative capillary pressure curve from MWX-1 is shown in Figure 5. Pc is capillary pressure and Sw is water saturation.

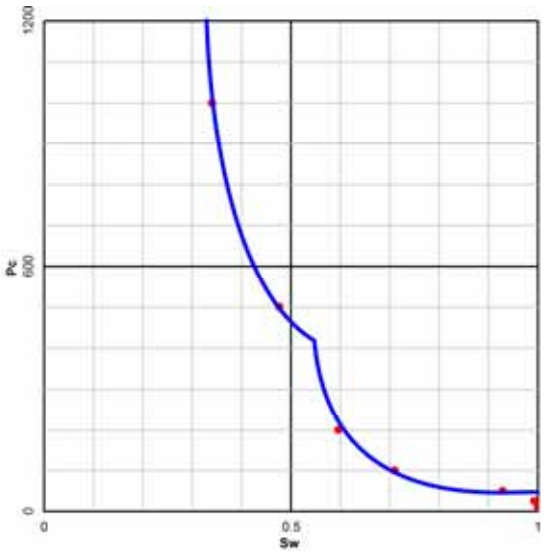

Figure 5: *Example capillary pressure curve from MWX-1 plotted in the standard way – capillary pressure vs. water saturation.*

When 1/Pc is plotted against Sw for each sample (Figure 6), it is clear that the range of data can be closely approximated by two intersecting straight lines.

Capillary pressure curves from other reservoirs show similar linear relationships, although the positions and slopes of the lines vary widely. This indicates that the capillary pressure curve is made up of two hyperbolae, even though the differences between the two are often difficult to observe on a linear Pc-Sw cross-plot.

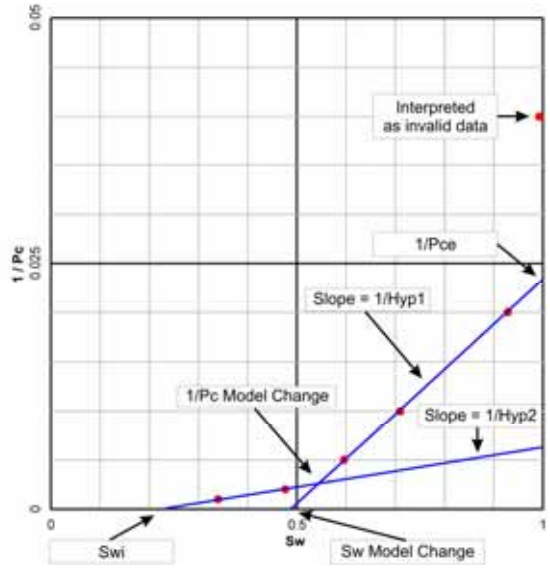

Figure 6: *Plot of reciprocal capillary pressure for example of Figure 5 to show how the elements of a capillary pressure curve are chosen (Figure 7).*

From these observations, a general model is proposed whereby any one capillary pressure curve can be expressed by six components (Figure 7):

- Pore entry pressure – equivalent to the largest pore throat of the rock; here termed Pce.
- An hyperbola describing the distribution of the larger pore network; here termed Hyp1.
- A discontinuity (often quite subtle) separating the larger pore network from a smaller pore network. For these rocks, this discontinuity perhaps separates solution porosity from inter-granular porosity. The capillary pressure value is termed Pc model change, or Pcmc, and the saturation value Sw model change, or Swmc. These two values have only a minor influence on the resulting capillary pressure model.
- An hyperbola describing the distribution of the small pore network; here termed Hyp2.
- Irreducible water saturation at high capillary pressure values and the theoretical minimum water saturation regardless of structural elevation above the hydrocarbon/water contact; here termed Swi.

These 6 numbers – Pce, Hyp1, Pcmc, Swmc, Hyp2, Swi – precisely describe the shape of the specific capillary pressure curve. Since Pc can be converted to height above zero capillarity, using appropriate laboratory/reservoir fluid properties, the 6 numbers can yield a precise saturation/height profile for the specific sample.

From the MWX-1 and MWX-2 wells there are 17 capillary pressure measurements available. Each sample has a different value for the 6 variables, as well as different porosities and permeabilities. Figure 8 shows interpretation procedures for 9 of the capillary pressure curves from the MWX-1 and MWX-2 wells. The basis of the model is integration of these data.

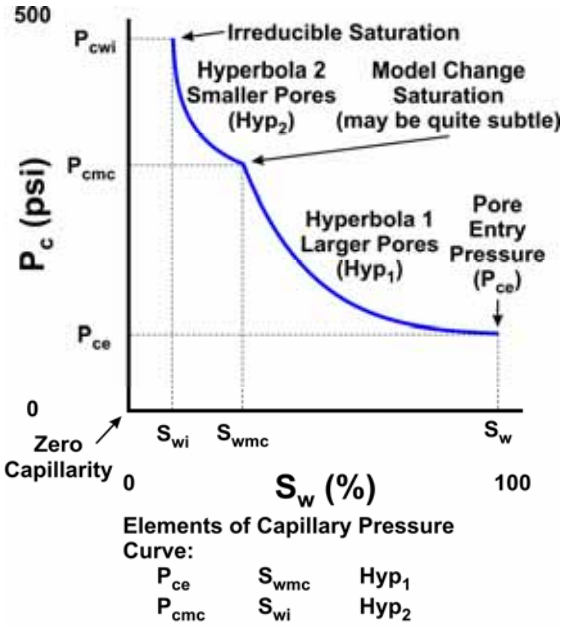

Figure 7: *Elements of a Capillary Pressure Curve.*

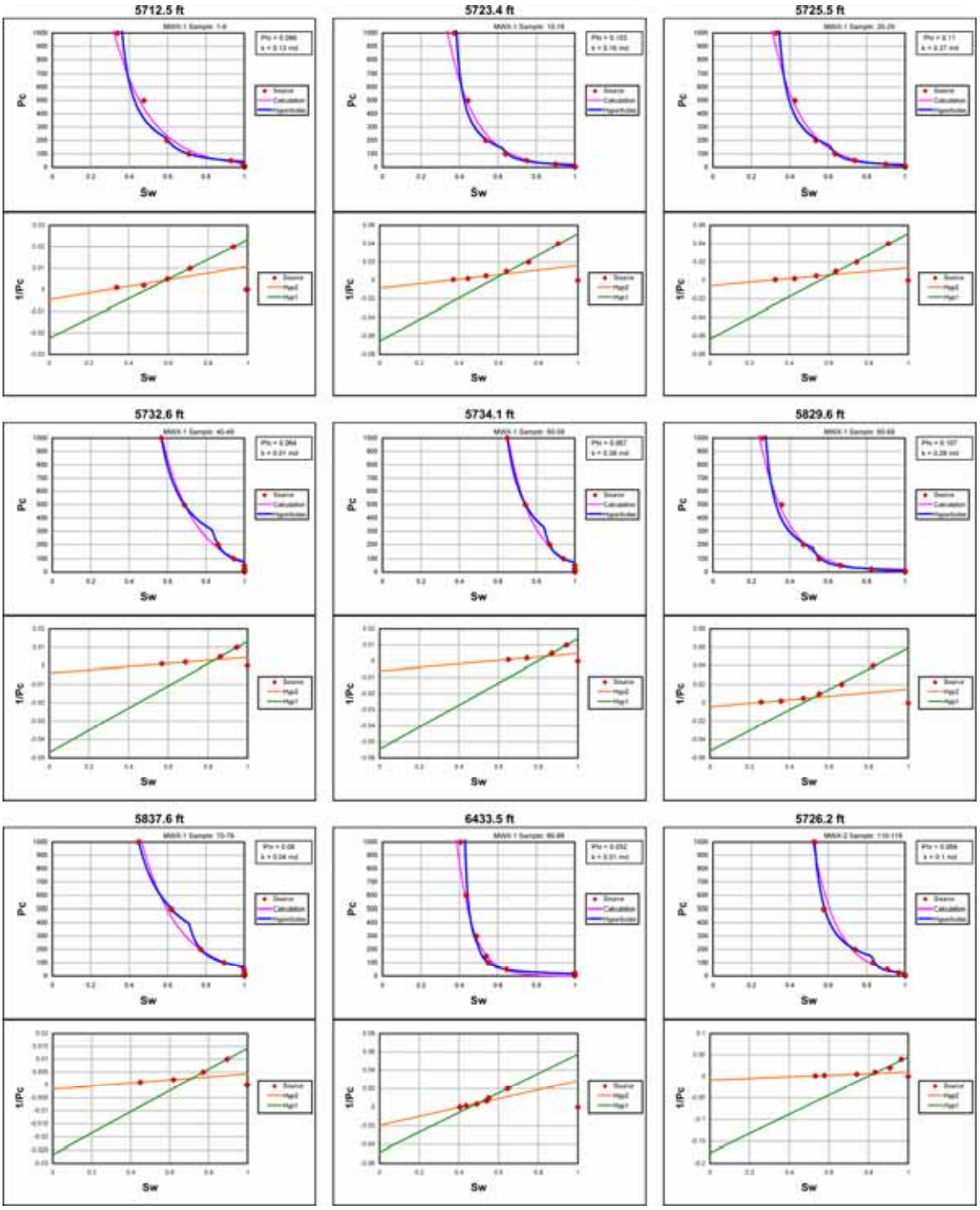

Figure 8: *Examples of 9 capillary pressure curves from MWX-1 and MWX-2 wells showing the interpretation procedures.*

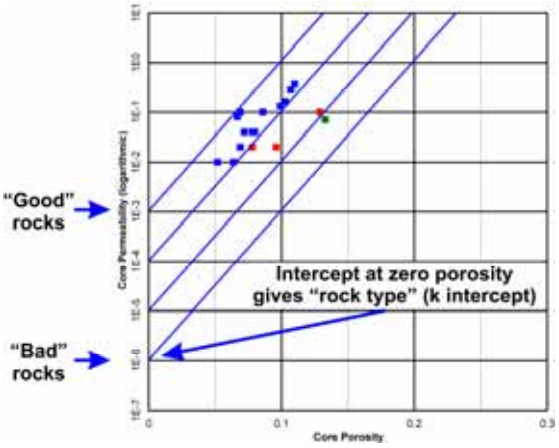

Figure 9: *Porosity vs. permeability cross-plots for MWX-1 showing distinction of "rock types."*

Figure 9 is a cross-plot of porosity vs. permeability. There is data scatter in the plot and it is suggested that different rock types will group such that the slope is similar, but the intercept on the zero porosity axis varies. Empirical relations involving permeability relations to porosity and irreducible water saturation include Timur (1968) and Coates et al (1997). Both models suggest correlations between porosity and permeability of about 3 decades of permeability increase for each 10% porosity increase. Many reservoirs where rock types are recognized show similar patterns (AAPG Memoir 71, 1999). Thus, a "rock type" can be defined on the basis of the permeability intercept at a specify value of zero porosity; the higher the value of the intercept, the "better" the rock – i.e. for any given porosity, the higher the permeability. The "rock type" number, by itself, gives no indication as to the absolute value of either porosity or permeability. See Figure 10 for a schematic representation.

Figure 11 is a series of cross-plots of the 6 capillary pressure curve components vs. porosity. Although the alignment of data is not perfect, there are distinctive trends in each plot. In general, for any given value of porosity, the "rock type" decreases as each parameter increases (Pce, Hyp1, Swi, Pcmc, Hyp2, Swmc).

For each plot a pivot point on the zero porosity can be established; values of similar "rock type" have different slopes. Figure 12 shows comparisons of the slopes of the correlations of Figure 11, compared with "rock type," and is the basis of the saturation/height model. Each reservoir will have a different set of correlations.

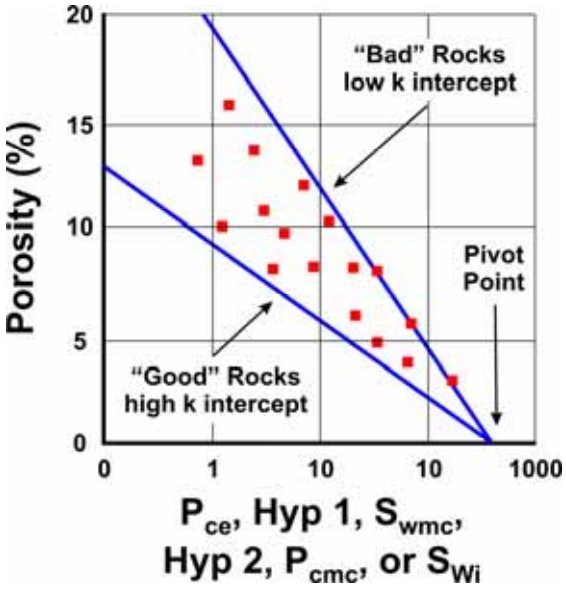

Figure 10: *Schematic diagram showing comparisons between capillary pressure curve elements and porosity for a series of capillary pressure curves.*

Procedures to compare with the petrophysical analyses are as follows:

1. Run standard petrophysical analysis to define effective porosity and water saturation profiles for the entire well.
2. Choose the hydrocarbon/water contact for the gross interval believed to belong to a single hydraulic unit. Use trends of downward-increasing Sw to help in this choice.
3. For each level in the hydraulic unit, knowing porosity, a series of theoretical saturation curves can be defined for the entire range of "rock types" using the correlations shown on Figure 12. At each level, height above the hydrocarbon/water contact is known, and therefore the location of the saturation data point for each possible "rock type" – at irreducible saturation, or within the hydrocarbon/water transition zone – is known.
4. Observe where the actual Sw curve (from petrophysical analysis) crosses the family of theoretical curves. The crossing point will give the "rock type" for that level. Figure 13 is a schematic of this methodology.

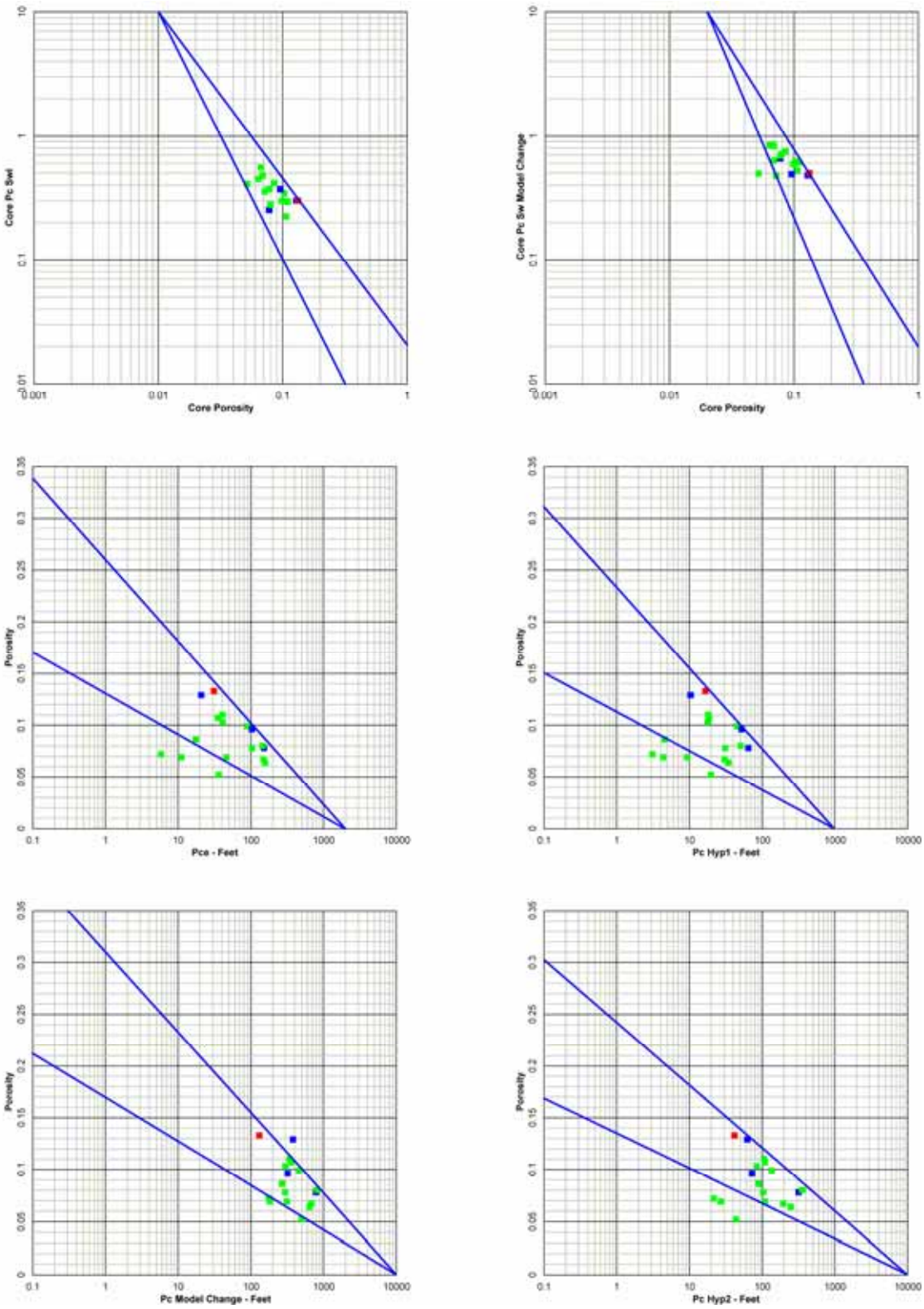

Figure 11: *Porosity vs. capillary pressure elements for samples from MWX-1 and MWX-2 wells.*

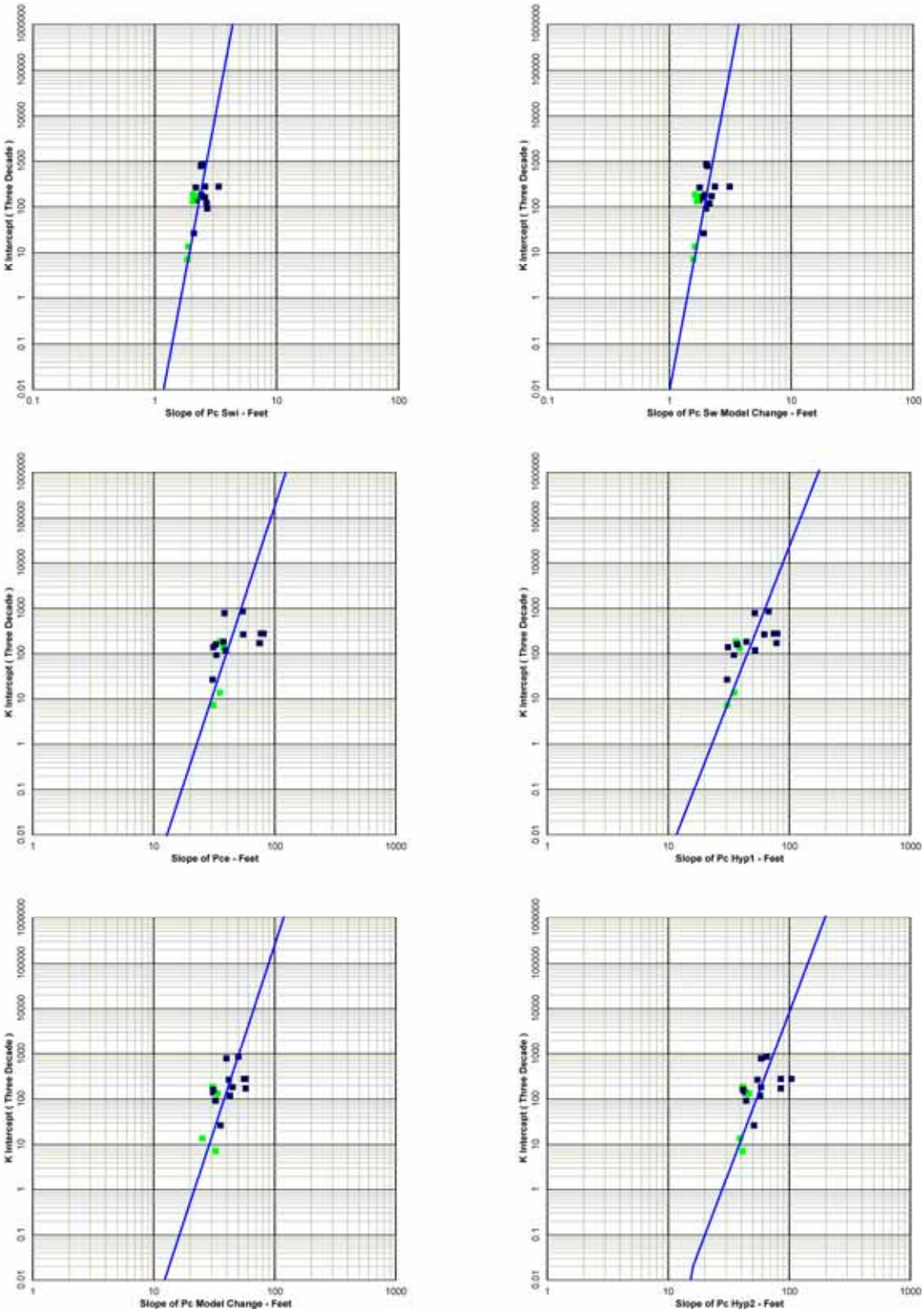

Figure 12: *Slopes of capillary pressure elements vs. "rock types" for samples from MWX-1 and MWX-2 wells.*

5. Knowing "rock type" and porosity, for each level, permeability can be calculated.
6. Using normalized hydrocarbon/water relative permeability curves, and knowing Sw at each level, relative permeability to each fluid phase can be estimated.
7. From total permeability and relative permeability, estimated effective permeability to each fluid phase is determined, level-by-level.

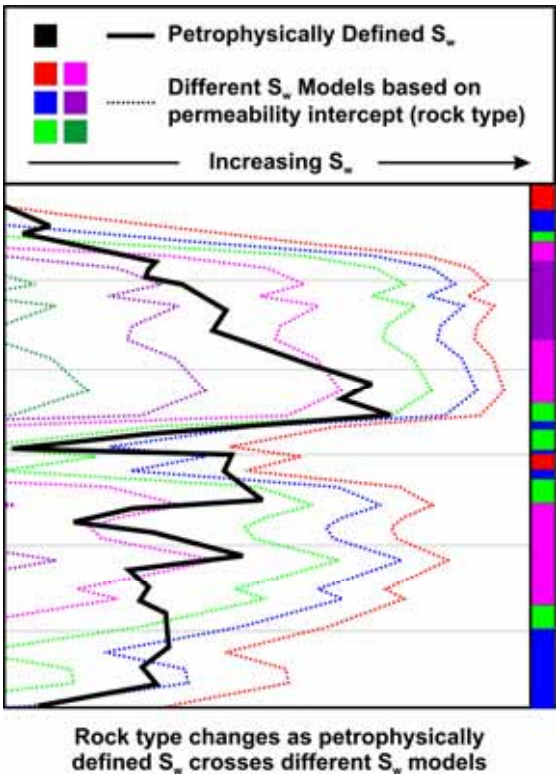

Figure 13: *Schematic of the capillary pressure/petrophysical model.*

DATABASE

We analyzed a good digital log suite from ten wells from Grand Valley, Paradise and Rulison Fields, kindly provided by Williams Production RMT Co. In addition to density/neutron logs on all wells, three wells have acoustic logs. Perforations, formation tops, and EUR data were also provided by Williams. Three wells from the MXW (Rulison) area are available from a GRI database (GRI/DOE Multi-Site Hydraulic Fracture Diagnostics Project, 1999).

RESULTS OF TRANSITION ZONE ANALYSIS

For the sandstones within the transition zone it can be shown that a minimum Rw of about 0.15 ohm-meter applies; see an example porosity/resistivity cross-plot for well GM 323-28 (Figure 14). This value of Rw applies only to gas-bearing intervals. As a consequence, any wet sands, with higher Rw, will give spurious gas saturation calculations. Figure 15 (from well GM 323-28) shows a comparison of:

- Water saturation, Sw Rlog, using traditional resistivity shaley formation analysis and the minimum Rw of 0.15 ohm-meter throughout.
- Water saturation estimates from the density and neutron pseudo logs (Sw Philog).

When Sw Rlog is approximately the same as Sw Philog it is reasonable to assume the sand is indeed gas-bearing; when Sw Philog is close to unity and larger than Sw Rlog, a wet sand is suggested with Rw more than 0.15.

This comparison has been applied to all wells, and Figure 16 is a cross-section highlighting the distinctions between gas-bearing and wet sands within the transition zone.

It is clear from the cross-section that there are significant volumes of gas above the top continuous gas column (KMV Gas). A challenge to completion engineers is whether or not these isolated gas sandstones can be stimulated without connecting to adjacent wet sandstones.

CAPILLARY PRESSURE RESERVOIR ANALOGUE

There is no well-defined downdip gas/water contact for the Williams Fork Sandstone package. All variations in porosity/saturation relations are believed to be a consequence of changing rock properties, not controlled by height above a gas/water contacts (if included such a contact exists). Figure 17 is an example of our capillary pressure model from MWX-1; good comparison exists between calculated permeabilities from the model and core measured permeability. This analysis suggests a valid model has been established for this part of the Piceance Basin, and

can be applied with confidence to wells with no cores.

Figure 18 shows examples among three wells of reservoir variation as defined by capillary pressure/petrophysical modeling. For all wells, intervals categorized to be of higher permeability were perforated. Other gas-bearing sandstones identified in this study to be of lower permeability, and probably non-commercial were also solutions perforated.

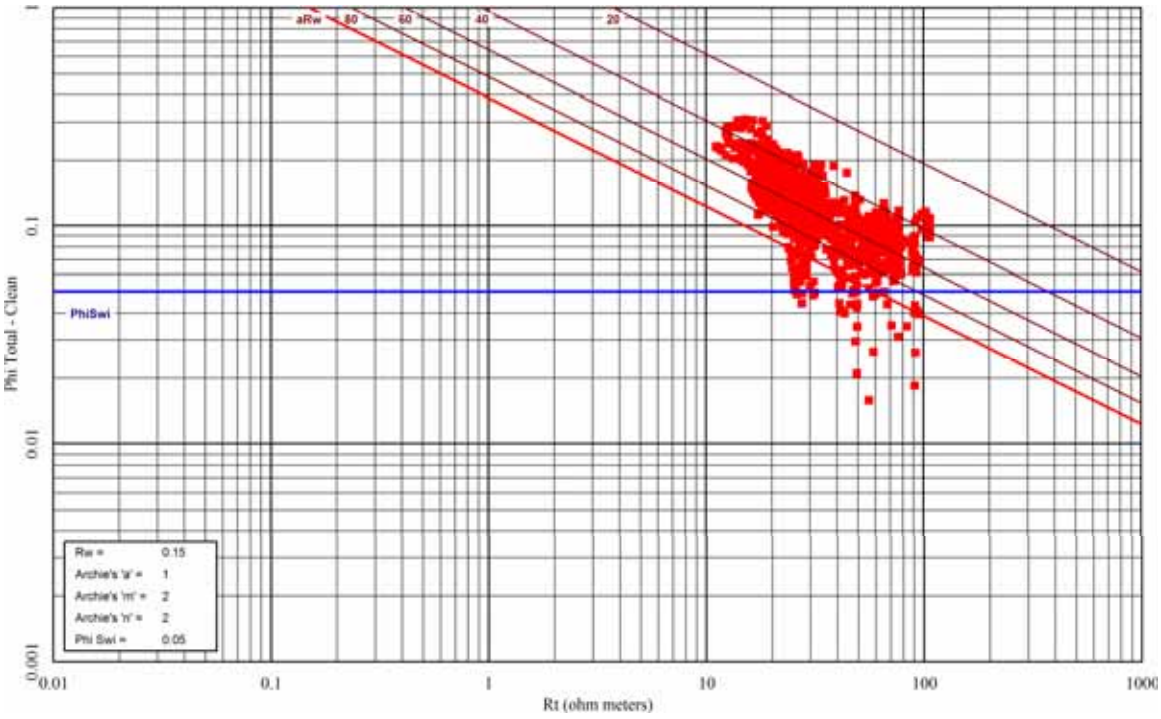

Figure 14: *Porosity/resistivity cross-plot – part of the transition zone well GM 323-28.*

A listing by well of EUR, gas occupied void volume, and permeability x thickness established from logs is shown in Table 2.

Figure 19 is a cross-plot of $k \times h$ vs. $Phi \times h \times Sg$ with values of EUR included, and Figure 20 is a cross-plot of $Phi \times h \times Sg$ vs. EUR with the values of $k \times h$ included. Patterns of the correlations indicate:

- EUR generally increases as $Phi \times h \times Sg$ increases
- $k \times h$ (sandstone matrix) increases $Phi \times h \times Sg$ as increases

Generally, $k \times h$ (sandstone matrix) increases with increasing EUR

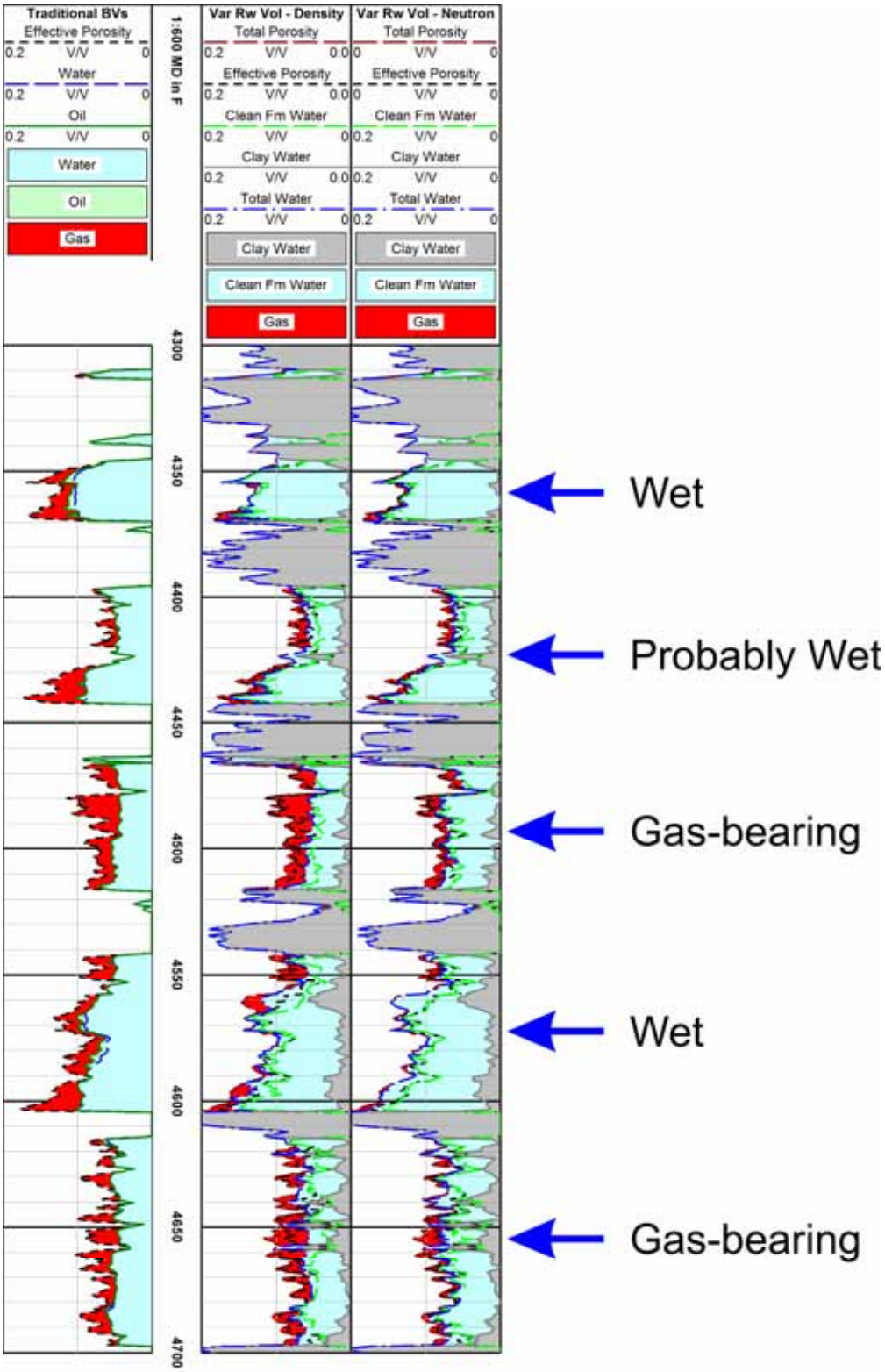

Figure 15: *Plot for part of the transition interval of GM 323-28 showing comparison between*

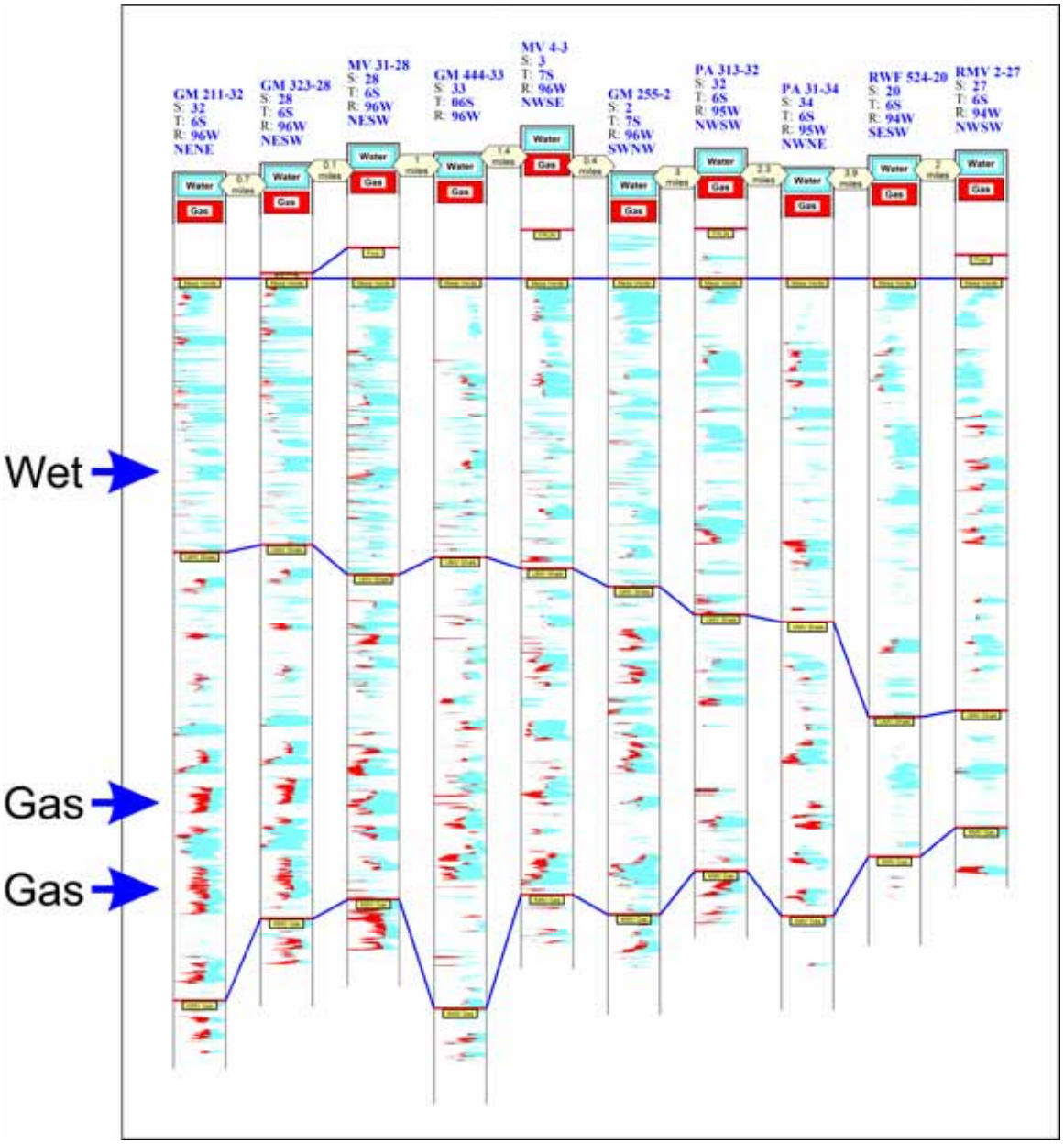

Figure 16: *Cross section of 10 wells showing the distribution of gas and water in the transition zone.*

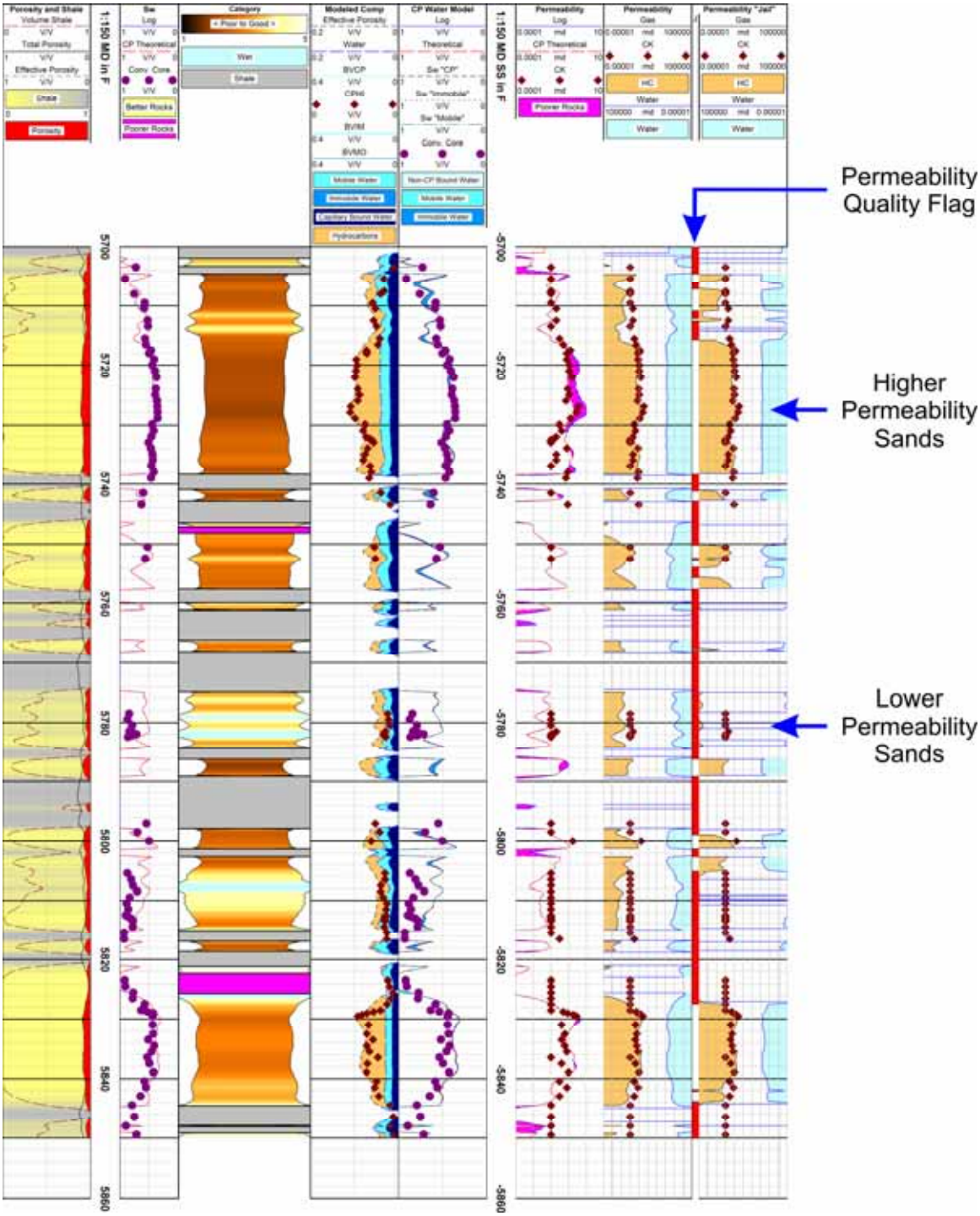

Figure 17: *Capillary pressure modeling combined with Petrophysics to show rock type recognition, the "permeability jail," and petrophysical/core data comparison.*

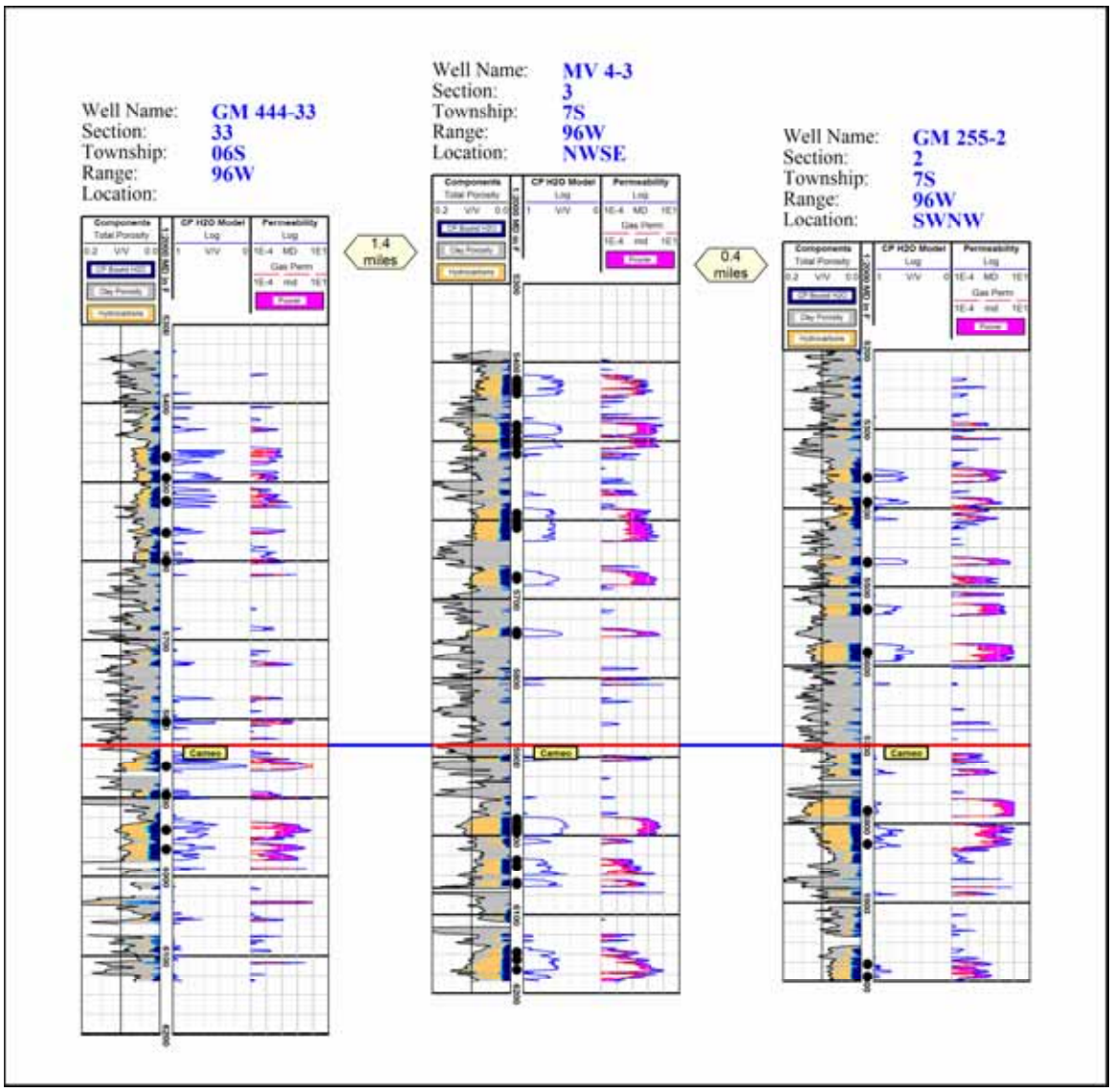

Figure 18: *Details of reservoir variation, as defined by capillary pressure/petrophysical modeling, for 3 wells in the continuous gas column.*

Well	EUR (BCF)	Phi*h*Sg (ft)	k*h (md ft)
GM 323-28	2.00	15.0	13.5
MV 31-28	1.97	18.0	22.0
GM 211-32	1.24	12.5	7.0
GM 444-33	0.91	8.0	8.0
MV 4-3	2.12	24.0	13.5
GM 255-2	1.10	10.5	9.0
PA 313-32	1.14	22.0	22.0
PA 31-34	1.38	13.5	19.0
RWF 524-20	1.75	11.5	14.0
RMF 2-27	3.52	19.5	21.0

Table 2: *Comparison of EUR with gas-occupied void volume from logs.*

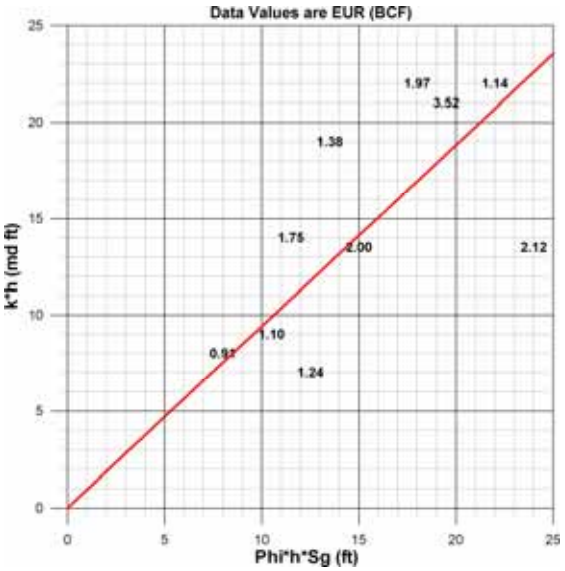

Figure 19: *Permeability x thickness (logs) vs. gas-occupied void volume (logs) – EUR in the Z direction.*

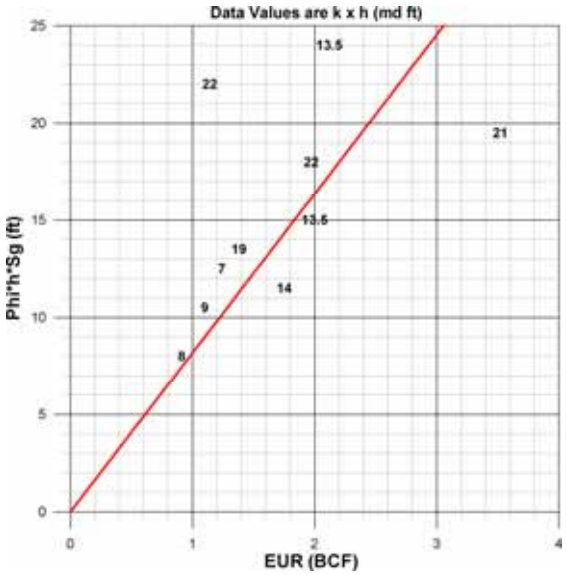

Figure 20: *Gas-occupied void volume (logs) vs. EUR – Permeability x thickness (logs) in the Z direction.*

CONCLUSIONS

A technique has been developed to distinguish fresh water wet sandstones from gas-bearing sandstones in the upper part of the William Fork Formation. The basis of the technique is detailed analysis of density and neutron response to estimate gas saturation, independent of water resistivity. From correlations among the study wells, it appears that the wet sandstones are more laterally continuous than the gas-bearing sandstones. Accurate distinction between gas-bearing and wet intervals is important when wells are completed.

Another approach combines core-measured capillary-pressure measurements with petrophysics to recognize different rock categories in the main gas accumulation. From these rock categories, permeabilities to gas were calculated at each reservoir depth level. Cumulative flow capacities ($k \times h$) and storage capacities ($Phi \times h \times Sg$) were compared with estimated ultimate recoveries. A logical correlation of increasing storage capacity as EUR increases exists.

ACKNOWLEDGEMENTS

Stephen Cumella of Barrett Resources kindly provided digital log information, perforated intervals and EUR information on ten wells operated by Williams Production Company. Steve also gave valuable insight into the geologic controls of gas production from this reservoir.

Stephen Cumella of Barrett Resources and Pam Logan of Mineral Acquisition Partners offered valuable criticism to the initial draft of this paper.

REFERENCES

Adrams, R., 1999, Reservoir characterization: AAPG Memoir 71.

Byrnes, A.P., 2003, Aspects of permeability, capillary pressure, and relative permeability properties and distribution in low-permeability rocks important to evaluation, damage, and simulation: Rocky Mountain Association of Geologists and Rocky Mountain Region of Petroleum Technology Transfer Council – Petroleum Systems and Reservoirs of Southwest Wyoming Symposium.

Coates, G.R., D. Marschall, D. Mardon, and J. Galford, 1997, A new characterization of bulk irreducible using magnetic resonance: Presented at

the Annual Logging Symposium of the Society of Professional Well Log Analysts, Houston.

Cumella, S. and D. Ostby, October 2003, Geology of basin-centered gas accumulation, Piceance basin, Colorado: RMAG and AIPG Piceance Basin Field Symposium.

Doveton, J. H., 1994, Geologic log analysis using computer methods, AAPG Computer Applications in Geology, No. 2, p. 1-22.

Gassmann, F., 1951, Über die elastizität poröser edien: Vier. der Natur. Gesellschaft in Zürich, 96, 1-23.

GRI/DOE multi-site hydraulic fracture diagnostic project, Gas Research Institute, GRI-99/0117, May 1999.

Holmes, M., and S.P. Cumella, 2003, Reservoir categorization from petrophysical analysis – mesaverde sandstone of the Piceance basin, northwestern Colorado: RMAG and AIPG Piceance Basin Field Symposium.

Kasap, E., M. Altunbay, and D. Georgi, Flow units from intergrated WFT and NMR data, 1999, in R. Schatzinger and J. Jordan, eds., Reservoir Characterization – Recent Advances, AAPG Memoir 71, p. 179-190.

Kennedy, M. C., 2002, Solutions to some problems in the analysis of well logs in carbonate rocks, in M. Lovell and N. Parkinson, eds., Geological applications of well logs: AAPG Methods in Exploration No. 13, p. 61-73.

Martin, F.D., et al, Advanced reservoir characterization for improved oil recovery in a New Mexico Delaware basin project, 1999, in R. Schatzinger and J. Jordan, eds., Reservoir Characterization – Recent Advances, AAPG Memoir 71, p. 93-108.

Nevans, J.W., et al., An intergrated geologic and engineering reservoir characterization of the North Robertson (Clear Fork) unit, Gaines County, Texas, 1999, in R. Schatzinger and J. Jordan, eds., Reservoir Characterization – Recent Advances, AAPG Memoir 71, p. 109-124.

Schlumberger, 1995, Log Interpretation Charts, Chart CP-5.

Shanley, K.W., R.M. Cluff, J.W. Robinson, 2004, Factors controlling prolific gas production from low-permeability sandstone reservoirs: implications for resource assessment, prospect development and rick analysis: AAPG Bulletin, Vol. 88 No. 8, pp 1083-1121.

Shanley, K.W., R.M. Cluff, L.T. Shannon, and J.W. Robinson, 2003, Controls on prolific gas production from low-permeability sandstone reservoirs: insights and implications from the Green River basin: RMAG and Petroleum Technology Transfer Council (PTTC) Petroleum Systems and Reservoirs of Southwest Wyoming Symposium.

Timur, A., 1968, An investigation of permeability, porosity and residual water saturation relationships: SPWLA Logging Symposium Transaction.

ABOUT THE AUTHORS

Michael Holmes has a Ph.D. from the University of London in geology and a MSc. from the Colorado School of Mines in Petroleum Engineering. His professional career has involved employment with British Petroleum, Shell Canada, Marathon Oil Company and H.K. van Poollen and Associates. For the past 15 years he has worked on petrophysical analyses for reservoirs worldwide under the auspices of Digital Formation, Inc.

Antony M. Holmes has a BS in Computer Science from the University of Colorado. He has been involved with the development of petrophysical software for 15 years with Digital Formation, Inc., particularly with regards to the implementation of petrophysical analyses.

Dominic I. Holmes has a BS in Chemistry and a BS in Mathematics from the Colorado School of Mines. He has been involved with the development of petrophysical software for 15 years with Digital Formation, Inc., particularly with regards to the presentation of petrophysical information in a graphical format.